ELSEVIER

Physica B 272 (1999) 96–100

PHYSICA B

www.elsevier.com/locate/physb

Picosecond and femtosecond near-field optical spectroscopy of carrier dynamics in semiconductor nanostructures

Ch. Lienau*, V. Emiliani, T. Günther, F. Intonti, T. Elsaesser

Max-Born-Institut für Nichtlineare Optik und Kurzzeitspektroskopie, Rudower Chaussee 6, D-12489 Berlin, Germany

Abstract

Quasi-two-color femtosecond pump–probe spectroscopy and near-field scanning optical microscopy are combined to study the carrier dynamics in single semiconductor nanostructures. In temporally, spectrally and spatially resolved measurements with a time resolution of 200 fs and a spatial resolution of 200 nm, the nonlinear change in reflectivity of a single quantum wire is mapped in real space and time. The experiments show that carrier relaxation into a single quantum wire occurs on a 100 fs time scale at room temperature. First experimental evidence is given for carrier transport along the wire axis on a picoseond time and 100 nm length scale.

Keywords: Quantum wire; Near-field microscopy; Femtosecond spectroscopy

During the last few years there has been a continuously growing interest in the application of optical techniques offering subwavelength spatial resolution, such as near-field scanning optical microscopy [1,2], to the spectroscopy of semiconductor nanostructures. By bringing the resolution of all-optical techniques closer to the nanometer size of these objects, the investigation of single nanostructures becomes possible and new and detailed insights into their optical and electronic properties are obtained. Moreover, the combination of nanometer scale optics with the powerful tools of ultrafast spectroscopy – providing temporal resolution in the range of a few femtoseconds – offers exciting new perspectives for gaining detailed microsopic insights into dynamic processes in nanostructures. Specifically, real-space transfer, trapping and relaxation of photogenerated carriers in low-dimensional semiconductors are of interest from the viewpoint of fundamental physics as well as device applications. First experimental activities in this novel field of research have focused on combining ultrafast spectroscopy and near-field microscopy to studies of GaAs microdisks [3] and quantum wells [4], carrier diffusion in ion-implanted GaAs quantum wells [5] and exciton spin dynamics in magnetic heterostructures [6]. In this paper, we apply for the first time femtosecond near-field pump–probe spectroscopy to one-dimensional nanostructures. The nonlinear optical response from a *single* (3 1 1) GaAs quantum wire (QWR) structure is resolved in real space and time. We present evidence for ultrafast relaxation of carriers into the quantum wire at room temperature and for carrier transport along the wire axis.

* Corresponding author. Tel.: + 49-30-6392-1476; fax: + 49-30-6392-1489.

E-mail address: lienau@mbi-berlin.de (C. Lienau)

0921-4526/99/$ - see front matter
PII: S0921-4526(99)00252-5

Quantum wires with a lateral width of 50 nm and a thickness of up to 13 nm embedded in a 6 nm GaAs quantum well (QW) were grown on patterned GaAs (3 1 1)A substrates [7]. The total confinement energy in the lateral (y) direction has a value of about 60 meV. Wires and the embedding QW are part of a multilayer structure that consists of the GaAs substrate, a 50 nm GaAs buffer layer, a 50 nm $Al_{0.5}Ga_{0.5}As$ lower barrier, the QWR/QW layer, a 50 nm $Al_{0.5}Ga_{0.5}As$ upper barrier and a 20 nm GaAs cap layer (Fig. 1a (inset)) [8–10]. At 300 K, the sample is characterized by intense photoluminescence (Fig. 1a inset) from both the QW (peaked at 1.52 eV) and QWR region (peaked at 1.46 eV) [11].

Spatially resolved femtosecond studies were performed with pulses derived from a modelocked 80 MHz Ti : sapphire oscillator which provides sub-40 fs pulses tunable in the wavelength range from 800 to 870 nm. The laser output is split into a pump and a probe beam, each traveling through a separate prism setup for spectral shaping and group velocity dispersion compensation. Two different optical configurations are used. In a near-field pump/near-field probe geometry, both pump and probe pulses are transmitted through the same near-field fiber probe. In a far-field pump/near-field probe geometry, only the probe pulse is sent through the fiber while the far-field pump is focused to a spot size of about 30 μm. In both cases, the probe light reflected from the sample is collected in the far-field and detected with a photodiode. For suppression of background signals, pump and probe beams are mechanically chopped at frequencies $f_1 \approx 1.2$ kHz and $f_2 = 1.77^* f_1$, respectively, and the photodiode signal is recorded with a lock-in amplifier at the sum frequency $f_1 + f_2$. Near-field aperture probes are made by chemically etching single-mode optical fibers to a sharp taper.

First, the carrier-induced optical nonlinearity of a single quantum wire is spatially and spectrally isolated by tuning the probe to the QWR resonance at 1.46 eV. Here, both pump and probe are transmitted through the fiber probe. Excitation at 1.51 eV generates electron–hole pairs in high-lying QWR states, the embedding QW as well as the GaAs cap and substrate layers. This carrier injection gives rise to a spatially homogeneous decrease

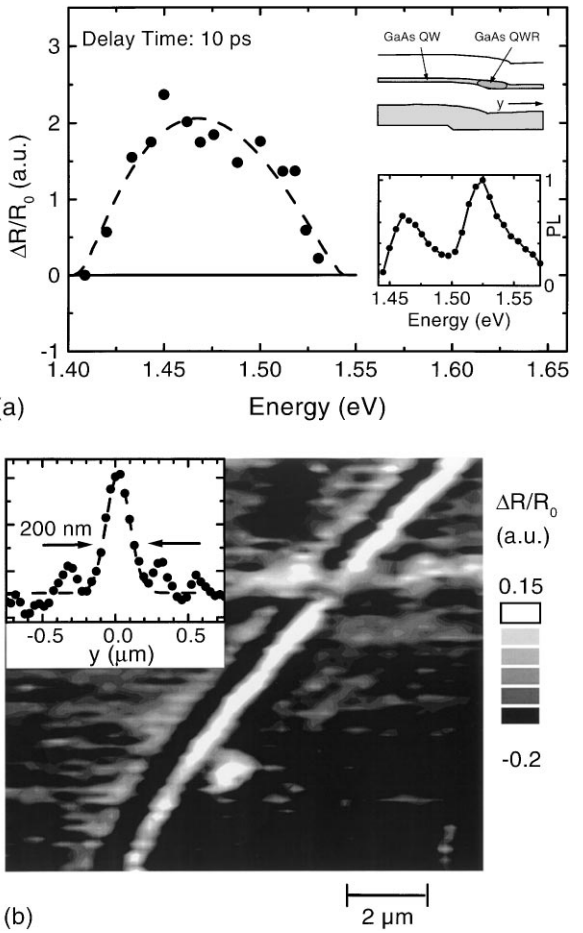

Fig. 1. (a) Probe wavelength dependence of the pump-induced quantum wire reflectivity change $\Delta R_{QWR}(t_d = 10\ \text{ps})/R_0$ (closed circles, excitation at 1.51 eV). Insets: schematic of the QWR sample and room temperature near-field PL spectrum. (b) Spatial map of the pump-induced reflectivity change $\Delta R/R_0$ at a delay time t_d of 10 ps. The pump and probe laser are set to 1.51 and 1.45 eV, respectively. Inset: line scan perpendicular to the wire axis for a pump energy of 1.48 eV.

in the reflectivity which is due to the GaAs cap and substrate layers. Superimposed on this background there is a pronounced increase in reflectivity that is localized at the QWR position at the sidewall of the [0 1 $\bar{1}$] mesa stripes. This position is independently identified from simultaneously recorded shear–force topography images. This local reflectivity peak is resolved with a spatial resolution of 200 nm which is limited by the finite distance between the

buried QWR and the sample surface (Fig. 1b, inset, in this scan the pump energy is slightly red-shifted to 1.48 eV). The variation of the reflectivity change $\Delta R_{QWR}/R_0 = (\Delta R(y=0) - \Delta R(|y| > 1\ \mu m))/R_0$ with probe energy E_{pr} is presented in Fig. 1a for a delay of 10 ps (solid circles). The reflection spectrum $\Delta R_{QWR}/R_0(E_{pr})$ is peaked around 1.47 eV, close to the maximum of the room temperature QWR PL spectrum. For excitation at a lower photon energy of 1.44 eV, where QWR absorption is negligible, the local reflectivity peak ΔR_{QWR} vanishes. These results demonstrate that the local reflectivity change ΔR_{QWR} reflects a change in the QWR susceptibility that is energetically localized to the excitonic QWR resonance.

To gain insight into the carrier dynamics of the QWR we follow the temporal variation of $\Delta R_{QWR}(t_d)$ for different excitation conditions. First, carriers are generated with a 50 fs far-field pulse with a spot size of 30 μm centered at 1.51 eV (Fig. 2b, inset). At this energy, a spatially homogeneous carrier distribution is generated in the GaAs cap and substrate, the QW and high-lying states of the QWR. The density generated by the pump pulse is set to 3×10^{11} cm^{-2}, ensuring non-degenerate excitation conditions. Probe pulses at 1.475 eV, near the QWR resonance, are transmitted through the fiber probe. On both sides of the QWR, a spatially homogeneous transient reflectivity decrease is observed that decays on a time scale of several picoseconds (Fig. 2a, open circles). This signal is dominated by the transient carrier-induced reflectivity change of the GaAs cap layer and the picosecond decay of the change of reflectivity reflects the trapping of carriers into surface states [12]. In contrast, a decrease in reflectivity with a smaller amplitude occurs at the QWR position $y = 0$. The QWR contribution, ΔR_{QWR}, is extracted by taking the difference of the two transients in Fig. 2a. The time evolution of ΔR_{QWR} (Fig. 2b) shows an ultrafast rise within 200 fs, the time resolution of the experiment, and remains nearly constant at later times. Similar transients are measured with pump pulses attentuated by a factor of 3.

Different dynamics are observed when both the pump and probe pulses are transmitted through the near-field fiber. Again, on both sides of the QWR, we observe the cap-layer-induced decrease in reflectivity that decays with a time constant of 2.5 ps (Fig. 3a, open circles). In contrast, at the quantum wire position, there is an increase in reflectivity for all positive delay times. The difference between both signals, ΔR_{QWR}, now shows a decay on a 10 ps time scale (Fig. 3b). Similar dynamics are observed for different probe energies between 1.48 and 1.43 eV and for resonant QWR excitation. The excitation density in these experiments was close to the one chosen for far-field excitation (Fig. 2).

In the experiments presented in Fig. 1 the carrier-induced change in the reflectivity of a single

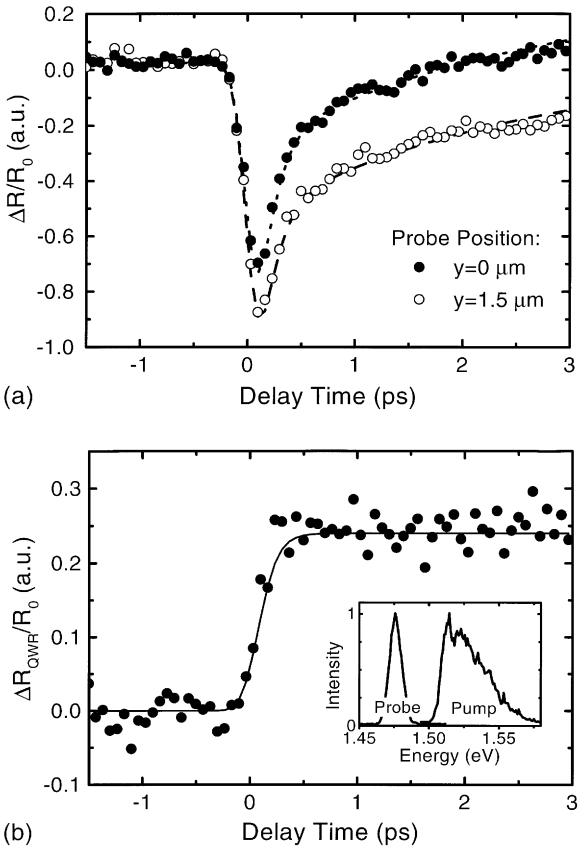

Fig. 2. (a) Temporal variation of $\Delta R/R_0$ at fixed spatial probe positions of $y = 0$ (QWR position, closed circles) and on the mesa top part at $y = 1.5$ μm. Excitation is with a far-field spot having a diameter of about 30 μm. (b) Temporal variation of the pump-induced change of the QWR reflectivity $\Delta R_{QWR}(t_d)/R_0 = (\Delta R(y=0, t_d) - \Delta R(y=1.5\ \mu m, t_d))/R_0$. Inset: spectra of pump and probe lasers.

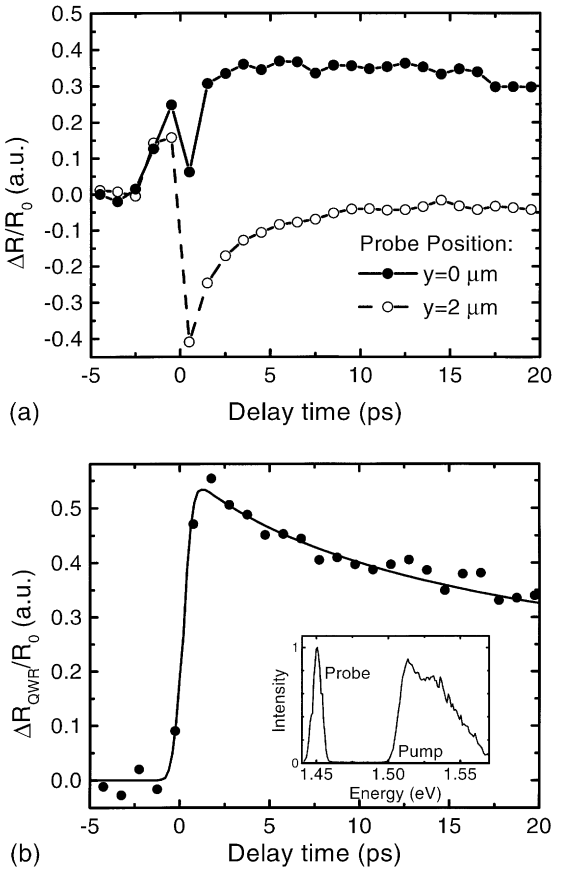

Fig. 3. (a) Temporal variation of $\Delta R/R_0$ at fixed spatial probe positions of $y = 0$ (QWR position, closed circles) and on the mesa top part at $y = 2\,\mu m$. Localized excitation is achieved by sending the pump laser through the near-field probe. (b) Temporal variation of the pump-induced change of the QWR reflectivity $\Delta R_{QWR}(t_d)/R_0 = (\Delta R(y = 0, t_d) - \Delta R(y = 2\,\mu m, t_d))/R_0$. Dashed line: simulation assuming one-dimensional diffusion along the wire axis with a diffusion coefficient $D_{QWR} = 20\,cm^2/s$. Inset: spectra of pump and probe lasers.

quantum wire is spatially and spectrally isolated with 200 nm spatial resolution. We observe a local increase in reflectivity that is energetically localized at the QWR resonance. This increase in reflectivity, ΔR_{QWR}, reflects a decrease in the absorption, i.e. the imaginary part of the susceptibility, around the QWR resonance. This interpretation is confirmed by a numerical simulation based on the matrix inversion method [13] and a transfer matrix formalism. The analysis indicates that the signal is less sensitive to changes in the refractive index. For the cap layer contribution, however, the negative sign of the reflectivity change is mainly influenced by the carrier-induced change in refractive index, i.e. the real part of the susceptibility, at the sample surface.

The QWR signal ΔR_{QWR} is sensitive to the concentration and energy distribution of carriers in the QWR. For far-field excitation at $E_{pump} > 1.51\,eV$ (Fig. 2) carriers are excited into both high-lying QWR states and into the surrounding QW. Probing at $E_{pr} = 1.46\,eV$, i.e. at the bottom of the quantum wire, one observes a rise in ΔR_{QWR} within the time resolution of 200 fs and a constant amplitude at longer times. There are two mechanisms contributing to this behavior: (i) screening of the excitonic contribution to the QWR absorption by optically injected carriers and (ii) band filling due to a carrier population in the low-lying states of the QWR. In quantum wells both effects are of similar magnitude [14], while in strongly confined one-dimensional structures screening is expected to be significantly reduced [15]. Due to the short-range nature of the exciton screening [16] the strength of both effects is a sensitive probe of the *local* carrier concentration within the QWR region. The first mechanism rises with the optically generated carrier concentration, i.e. follows instantaneously the time integral of the pump pulse. In contrast, the second mechanism requires carrier redistribution from optically excited high lying states to the bottom of the QWR. The absence of any slower dynamics on the transients in Fig. 2b suggests that this redistribution process occurs within the first 200 fs. This relaxation involves a complex scattering scenario between high-lying QWR states and states at the bottom of the QWR. From the efficiency of this relaxation we conclude that in addition to carrier–LO phonon scattering, carrier–carrier scattering is playing a dominant role under our experimental conditions. The diffusive transport of carriers excited in the QW into QWR occurs on a much slower time scale [10] and does not affect the signal within the first few picoseconds.

For far-field excitation with a 30 μm spot size, a homogeneous carrier distribution is generated along the wire axis. Motion of carriers along the wire axis is not expected to affect the reflection signal. In fact, the decay time of reflectivity change

is expected to be equal to the PL decay time, which is 1.9 ns at room temperature [8]. This is different for near-field excitation through the fiber probe (Fig. 3). Here, the excitation and probe pulses are spatially overlapping and are localized to a small spot of about 300 nm dimension. Thus migration of carriers out of the excitation volume leads to a decrease in the local carrier concentration and – thus – to a reduction in the pump-induced reflectivity change. This carrier migration is contributing to the decay of ΔR_{QWR} on a 10 ps time scale reported in Fig. 3. In general, the transport of carriers out of the excitation volume can occur both along the wire axis as well as perpendicular to the QWR axis. The large confinement energy of 60 meV represents a barrier that opposes the diffusive real-space transfer perpendicular to the QWR axis into the embedding QW. This results in strongly different time scales for the carrier transport along the two orthogonal directions and makes our experiment mainly sensitive to the carrier transport along the wire direction. Assuming that the transport along the wire axis – on timescales of several picoseconds – is adequately represented within a drift–diffusive model, we find that the observed decay of the pump-induced change in QWR reflectivity is well described by taking an ambipolar diffusion coefficient $D_{QWR} = 20\ cm^2/s$ (dashed line in Fig. 3b). This value is slightly larger than the corresponding 2D room temperature diffusion coefficient $D_{QW} = 12\ cm^2/s$ found for this sample [8]. This analysis suggests that during the first 20 ps, the width of the carrier distribution along the wire axis increases from about 350 to more than 700 nm.

In conclusion, we have demonstrated, for the first time, the potential of femtosecond near-field spectroscopy for directly imaging the carrier dynamics in a single semiconductor nanostructure. By combining ultrahigh spatial and temporal resolution we have resolved the ultrafast relaxation of carriers into a single QWR on a 100 fs time scale at room temperature. First evidence has been given for the diffusive transport of photogenerated carriers along the wire axis on a picosecond time and 100 nm length scale.

Acknowledgements

This work was supported by the Deutsche Forschungsgemeinschaft (SFB 296) and the European Community (Ultrafast Quantum Optoelectronics Network). V.E. gratefully acknowledges a Marie-Curie fellowship. The high-quality QWR samples have been provided by Richard Nötzel and Klaus Ploog.

References

[1] D.W. Pohl, W. Denk, M. Lanz, Appl. Phys. Lett. 44 (1984) 651.
[2] E. Betzig, J.K. Trautman, Science 257 (1992) 189.
[3] J.B. Stark, U. Mohideen, E. Betzig, R.E. Slusher, Ultrafast Phenomena IX, Springer Series in Chemical Physics, Springer, Berlin, 1996, p. 349.
[4] S. Smith, N.C.R. Holme, B. Orr, R. Kopelman, T. Norris, Ultramicroscopy 71 (1998) 213.
[5] B.A. Nechay, U. Siegner, F. Morier-Genoud, A. Schertel, U. Keller, Appl. Phys. Lett. 74 (1999) 61.
[6] J. Levy, V. Nikitin, J.M. Kikkawa, A. Cohen, N. Samarth, R. Garcia, D.D. Awschalom, Phys. Rev. Lett. 76 (1996) 1948.
[7] R. Nötzel, M. Ramsteiner, J. Menniger, A. Trampert, H.-P. Schönherr, L. Däweritz, K.H. Ploog, Jpn. J. Appl. Phys. 35 (1996) L297.
[8] A. Richter, G. Behme, M. Süptitz, Ch. Lienau, T. Elsaesser, M. Ramsteiner, R. Nötzel, K.H. Ploog, Phys. Rev. Lett. 79 (1997) 2145.
[9] Ch. Lienau, A. Richter, G. Behme, M. Süptitz, D. Heinrich, T. Elsaesser, M. Ramsteiner, R. Nötzel, K.H. Ploog, Phys. Rev. B 58 (1998) 2045.
[10] A. Richter, M. Süptitz, D. Heinrich, Ch. Lienau, T. Elsaesser, M. Ramsteiner, R. Nötzel, K.H. Ploog, Appl. Phys. Lett. 73 (1998) 2176.
[11] A. Richter, M. Süptitz, Ch. Lienau, T. Elsaesser, M. Ramsteiner, R. Nötzel, K.H. Ploog, Surf. Interface Anal. 25 (1997) 583.
[12] J.J. Baumberg, D.A. Williams, K. Köhler, Phys. Rev. Lett. 78 (1997) 3358.
[13] S. Schmitt-Rink, C. Ell, H. Haug, Phys. Rev. B 33 (1986) 1183.
[14] J.B. Stark, W.H. Knox, D.S. Chemla, Phys. Rev. Lett. 68 (1992) 3080.
[15] S. Benner, H. Haug, Europhys. Lett. 16 (1991) 579.
[16] S. Schmitt-Rink, D.S. Chemla, D.A.B. Miller, Phys. Rev. B 32 (1985) 6601.